THE ANOMALY DETECTION EFFICIENCY OF KERNEL DENSITY ESTIMATION FUNCTIONS ON UAV IMAGES

Nguyen Van Phuong[1], *Dao Khanh Hoai*[2], *Tong Minh Duc*[1]

Abstract

The anomalous pixel detection efficiency of algorithms on UAV images is represented by the two criteria: anomalous pixel detection effect (which uses the area under ROC curve for evaluation) and calculation time. A highly effective researcher-recommended technique for anomaly detection on UAV images is to apply Neyman-Pearson lemma by calculating Kernel Density Estimation (KDE) for background data and making decision therefrom. In this method, the selection of kernel function and bandwidth plays the determinant role in anomaly detection efficiency. However, there has not been any research that mentions this issue to date. Hereby, in this study, we evaluate anomaly detection efficiency on UAV images through a number of common kernel functions typically cited in researches on KDE, and follow up with making recommendations for appropriate uses of kernel functions. Experiments and evaluations are carried out on the sample data set photographed on varied terrain types and objects of interest.

Index terms

Nonparametric density estimation, KDE, Kernels, UAV images, search and rescue

1. Introduction

Search and rescue operations include searching and rescuing human and vehicles trapped in adverse situations. An increasingly adopted tool is using high-definition images shot from a payload on unmanned aerial vehicle (UAV) [1], [2]. This equipment is truly a great resource for search and rescue mission [3], [4] as it can carried sensors to acquire high-definition images spanning a vast operational range, varied terrains, without calling for too much human resource and expense for search and rescue operations. Notwithstanding, a barrier that challenges manual search arises from the fact that sensors have to scan on a vast area, the size of a missing person or object of interest is very small compared to the scene and easily mixed with background data. Manual search sometimes does not guarantee time and subsequently lessens the victim's chance of survival. Automatic target detection techniques on UAV images [5], [6], [7], [8] can support and accelerate this process.

[1]Faculty of Information Technology, Le Quy Don Technical University, [2]Geodesy and Mapping Department, Le Quy Don Technical University

Automatic target detection based on geometrical features can be used as an approach to this issue; however, geometrical features of objects of interest remain unspecified in most of search and rescue cases due to receiver's capturing angle, or search objects partly hidden by terrain or high density of leaves, or partly submerged in water. Directly finding out the victim is most ideal, but in some cases, objects like clothes, blanket, tent, personal items, vehicle's fragments and so on can provide helpful information. Hereby, anomaly detection (or outlier) will serve as a more appropriate approach to this issue. Anomalies on UAV images are identified as pixels or clusters of pixels with conspicuous or highly varied colours compared to surrounding pixels. These pixels are thinly scattered and rarely representative of the image. Generally, signals for anomalies are spatially small and exist at a low probability in an image.

In the year 2012, 2013 and 2015 [5], [6], [7], the group of researchers from Boston University, USA worked on some techniques for detecting outlier colour on UAV images applied in search and rescue operations. The first technique is to test binary hypothesis in order to detect anomalous pixels [5]. For this method, the authors applied Neyman-Pearson lemma by calculating non-parametric probability density of background data to make decision. For the second technique [6], M. Ramachandran and W. Moik proposed using K-Mean algorithm to sort pixels into clusters. All pixels in a cluster are identified as normal if the number of centers of surrounding clusters covered by an area within the radius R (from the center of the present cluster) is higher or equal to N_{max}. Conversely, all pixels in the present cluster are anomalous ones. The third technique [7], relates to the principal component analysis gaps. The anomaly detector determines gaps between clusters along the vector of greatest variability, searches for the largest area along a vector individually to isolate a set of anomalous pixels. The fourth technique [5], [6], [7], the authors tested the ability to detect anomalies on UAV images of RX algorithms [9] and some its variations such as: the dual window-based eigen separation transform, the nested spatial window-based target detection. Results from researches showed that images captured from UAV are able to serve search and rescue operations. Outlier pixel detection rates (these pixels might contain helpful information for search and rescue operations) of algorithms on the sample data set were all over 95%. In the research [8], authors surveyed outlier colour detection ability of RX [9] and its variations across eight colour spaces from UAV images. It showed that using appropriate colour space will deliver satisfactory results, which could support detection of informative objects for search and rescue operations.

For the first technique, researchers applied Neyman-Pearson lemma by calculating probability density function (PDF) through estimating kernel density of background data and follow-up decision making. In 2011, Veracini and associates [11] used Parzen Window (PW) method [12] to calculate background PDF using Gaussian kernel density estimation function, and a reliable result was achieved. The background PDF, achieved through PW approximation, was used as the input to detect anomalies on images through binary hypothesis testing method. In 2014, similar to Veracini's method, Matteoli and associates [13] selected Gaussian kernel function with a fixed bandwidth to calculate probability density function, then applied Neyman-Pearson lemma to sort pixels into

Table 1. A number of typical kernel functions [10]

Tên nhân	$K(u)$	Điều kiện
Uniform (Uni)	$\frac{1}{2}$	$\|u\| \leq 1$
Hypercube (Hyp)	1	$\|u\| \leq \frac{1}{2}$
Triangular (Tri)	$1 - \|u\|$	$\|u\| \leq 1$
Epanechnikov (Epa)	$\frac{3}{4\sqrt{5}} - \frac{3u^2}{20\sqrt{5}}$	$\|u\| \leq \sqrt{5}$
Quartic (Qua)	$\frac{15}{16}(1-u^2)^2$	$\|u\| \leq 1$
Triweight (Triw)	$\frac{35}{32}(1-u^2)^3$	$\|u\| \leq 1$
Tricube (Tric)	$\frac{70}{81}(1-\|u\|^3)^3$	$\|u\| \leq 1$
Gaussian (Gau)	$\frac{1}{\sqrt{2\pi}} e^{-\frac{1}{2}u^2}$	
Cosine (Cos)	$\frac{\pi}{4} cos\left(\frac{\pi}{2}u\right)$	$\|u\| \leq 1$

normal class or anomalous class. In 2017, Zhao and associates [14] combined PDF calculation through KDE using Gaussian kernel function with findings from correlation representation to detect anomalous pixels.

The Gaussian kernel function was applied in all of the above publications, and there was no explanation for why this kernel function was selected. Is there a kernel function that provides better rate rather than Gaussian kernel function? In addition, there was no calculation or explanation for selecting bandwidth for highest anomaly detection efficiency. Through experimental method, using the sample image set shot on varied terrain types and search objects to evaluate the anomaly detection rate for UAV images of some common kernel functions (see Table 1) that are typically cited in researches, quantitative research results, area under ROC curve, is the measurement for algorithm's anomaly detection efficiency. In addition, we analyse the effect from selecting varied bandwidths on kernel functions' anomaly detection efficiency.

In the following parts of this article, we will present these contents: Part 2- Strategy for detection of anomalies on UAV images, Part 3- Testing method, testing result analysis, evaluation, recommendation for appropriate kernel function, Part 4- Conclusion.

2. Strategy for detection of anomalous pixels on UAV images

Detection of anomalous pixels on UAV images applied in search and rescue operations is viewed as the task of sorting pixel into either "normal" class (C_1 class) or "anomalous" class (C_2 class). Take an multispectral image with L spectral bands, this image is formed by a collection of n pixels $\mathbf{X} = (\mathbf{x}_1, \mathbf{x}_2, ..., \mathbf{x}_n)$. The observation i on $\mathbf{X}$ is $\mathbf{x}_i = (\mathbf{x}_i^1, \mathbf{x}_i^2, ..., \mathbf{x}_i^L), i = 1, 2, ..., n$, to be able to sort $\mathbf{x}_i$ into *"normal"* or *"anomalous"* according to statistic method is to test binary hypothesis by using Neyman-Pearson based on likelihood rate (LR) of conditional probability density function by the two

hypotheses:

$$\hat{H}(\mathbf{x}_i) = \begin{cases} H_0 : \mathbf{x}_i & \in C_1; \\ H_1 : \mathbf{x}_i & \in C_2. \end{cases} \quad i = 1, 2, ..., n \tag{1}$$

According to Neyman-Pearson lemma, we have:

$$\wedge_{NP}(\mathbf{x}_i) = \frac{\hat{f}_{\mathbf{X}|H_1}(\mathbf{x}_i)}{\hat{f}_{\mathbf{X}|H_0}(\mathbf{x}_i)} \begin{matrix} H_1 \\ \geq \\ < \\ H_0 \end{matrix} \eta, i = 1, 2, ..., n \tag{2}$$

Whereof $\hat{f}(\cdot)$ is the conditional probability density function, η is the appropriate threshold to sort $\mathbf{x}_i$ into *"normal"* or *"anomalous"* class. However, in reality, parameters, used in calculation conditional probability density function in the formula (2) applied in search and rescue, are normally unavailable for we lack knowledge about *"anomalous"* class; moreover, anomalous pixels normally have a random spectral value that only depends on the images' scenes, they are independent pixels or clusters of pixels of very small size compared to images and their density is thin. Therefore, we can assume that $\hat{f}_{\mathbf{X}|H_1}(x_i)$ is a constant, then the formula (2) will be shortened as:

$$\wedge(\mathbf{x}_i) = -log\{\hat{f}_{\mathbf{X}|H_0}(\mathbf{x}_i)\} \begin{matrix} H_1 \\ \geq \\ < \\ H_0 \end{matrix} \eta, i = 1, 2, ..., n \tag{3}$$

Since the background data's probability density $\hat{f}_{\mathbf{X}|H_0}(\mathbf{x}_i)$ is unknown so it has to be estimated from existing data. With the assumption that there is only a very few number of thinly scattered anomalous pixels, all the pixels $\mathbf{x}_i \in \mathbf{X}, i = 1, 2, ..., n$ can be used for this estimation.

In researches [11], [13], [14], the authors used nonparametric probability density estimation method to estimate $\hat{f}_{\mathbf{X}|H_0}(\mathbf{x}_i)$ as we do not have to make any assumption about data distribution. In this method, its main tool is KDE, which was published by Rosenblatt in 1956 [15], later developed and published by Parzen in 1962 [12]. For unidirectional data, observe the random vector $\mathbf{x} = [x_1 x_2 \dots x_n]^T$ of the random variable $\mathbf{x}$ with n elements. This means that there are n observations for the random variable $\mathbf{x}$ and x_i is the i observation of the random variable $\mathbf{x}$. Then the kernel density estimation of the random variable $\mathbf{x} = [x_1 x_2 \dots x_n]^T$ is as follows:

$$\hat{f}(x_i) = \frac{1}{n} \sum_{j=1}^{n} \frac{1}{h_j} K\left(\frac{x_i - x_j}{h_j}\right), i = 1, 2, ..., n \tag{4}$$

Whereof, $\hat{f}(\cdot)$ is PDF, $K(u)$ is called multiplicative function that satisfies the condition $\int_{-\infty}^{\infty} K(u)d(u) = 1$ and h_j is the proportionality factor that decides the *"width"* of multiplicative function, or also known as bandwidth. Extended discussion on statistical

features of $\hat{f}(\cdot)$ can be found in [16], $K(u)$ can be typical multiplicative functions presented by Hardle in [10] shown in Table 1.

In case that data has k directions, the observation i of $\mathbf{X}$ will be $\mathbf{x}_i = [\mathbf{x}_i^1, \mathbf{x}_i^2, \ldots, \mathbf{x}_i^k]^T, i = 1, 2, \ldots, n$, the formula for estimating kernel density of multivariant data is defined in [10] as:

$$\hat{f}(\mathbf{x}_i) = \frac{1}{n}\sum_{j=1}^{n}\left\{\prod_{d=1}^{k}\frac{1}{h_d}K\left(\frac{x_i^d - x_j^d}{h_d}\right)\right\} \tag{5}$$

For UAV images, the data is of multivariant type, we will apply formula (5) to set up algorithm. By adopting the method of Matteoli et al. [13], we will fix the bandwidth, set $h = h_1 = h_2 = ... = h_d$ with $d = 1, 2, ..., k$. The algorithm 1 is simulated to sort pixels into C_1 class or C_2 class.

Algorithm 1: The algorithm for anomalous pixel detection

input: the matrix of pixels X, the number of pixels n, the number of channel k, bandwidth h, anomaly detection threshold η.

output: the collection of normal pixels C_1, the collection of anomalous pixels C_2.

$C1 \leftarrow \emptyset$;
$C2 \leftarrow \emptyset$;
for $i \leftarrow 1$ **to** n **do**
  $sum\_ker \leftarrow 0$;
  for $j \leftarrow 0$ **to** n **do**
    $mul\_ker \leftarrow 1$;
    for $d \leftarrow 1$ **to** k **do**
      $mul\_ker \leftarrow mul\_ker \times K(\frac{X_i^d - X_j^d}{h})$;
    end
    $sum\_ker \leftarrow sum\_ker$ + mul_ker;
  end
  if $\frac{sum\_ker}{n} \leq \eta$ **then**
    $C2 \leftarrow C2 \cup X_i$
  end
  else
    $C1 \leftarrow C1 \cup X_i$
  end
end

3. Experiment and evaluation

3.1. Experiment scenario

UAV image data acquired from actual search and rescue cases in Vietnam remains rare and basically unpublicized. In order to test research results, we carry out testing in under conditions: in terms of terrain types: plain, light forest, hill slope, lake and pond, coastal area. In terms of search objects, we use personal utensils (in rescue cases) such as cloths, life vest, life buoy, vehicle fragments (with size $\leq 30 \times 30cm$). The elevation of aerial vehicle is nearly 200m under daylight observation condition, with sunlight, regular observation camera. Specifically: we used three images published in the research "Some techniques for detection of anomalies on UAV images applied in search and rescue operations" [8]. The first image is shown in Fig. 1, shot on plain with Canon IXUS 127 HS camera at an elevation of 190m, ground resolution of 6.3cm/1 pixel; the second and the third image are shown on Fig. 2 and Fig. 3, they are shot on coastal area with Sony DSC-WX220 camera at an elevation of 200m, ground resolution of 64mm/1 pixel. Each image has the size of 1000×1000 pixels and provided with three different samples of anomaly depending on terrain types. The scene shot on plain (Image 1) and the scene shot on light forest (Image 2) were provided with three shirt samples of different sizes and colours on each image. The scene shot on coastal area (Image 3) were provided with two life vest samples with different colours, and a life buoy.

Fig. 1. The scene shot on plain, provided with three shirt samples of different sizes and colours (Image 1).

In addition, in the hill slope and lake & pond areas, we provide some clothes of different size and colours; some plastic pieces (that simulate vehicle fragments);

Fig. 2. The scene shot on light forest, provided with three shirt samples of different sizes and colours (Image 2).

Fig. 3. The scene shot on a coastal area, provided with two life vest samples with different colours and one life buoy (Image 3).

provided a life vest in a lake. Use flying equipment DJI Inspire 1 that carried camera X3 model FC350, flying at an elevation of 254, the ground resolution of 40mm/1 pixel. Fig. 4 is an image shot in the area provided with some clothes (Image 4). Fig. 5 is an image shot in the area provided with some plastic pieces which simulates vehicle fragments (Image 5) and Fig. 6 is an image shot in the area provided with life vest (we name it Image 6).

Fig. 4. The scene shot on an area provided with clothes of different sizes and colours (Image 4).

Fig. 5. The scenes shot in the area provided with some plastic pieces which simulates vehicle fragments (Image 5).

So the sample data set for testing includes images of 1,000,000 pixels that cover from 1,600m^2 to 4,000m^2 of terrain area, depending on each image. The corresponding kernel function of each image is used as shown in Table 1 with fixed bandwidth, similar to the method proposed by Matteoli et al. [13] for anomalous pixel detection. The anomaly detection efficiency of the method is calculated by the area under the ROC (Receiver Operating Characteristic). For each kernel function, we let the bandwidth h run from

Fig. 6. The scenes shot in the area provided with life vest (Image 5).

1 to 30, choose bandwidth for highest anomaly detection efficiency as the anomaly detection efficiency of kernel function. Apart from evaluation of anomaly detection efficiency of kernel functions, we evaluate the time duration for implementation and memory use of each kernel function.

The computer's configuration for calculation is as follows:

CPU: Intel Core i5-7400 3,00 GHz (4 core, 8 thread);

Mainboard: MSI B150M MORTAR ARCTIC;

RAM: DDR4 16GB;

HDD: SDD BIOSTAR S100 - 240GB;

Graphic: NVIDIA GeForce GTX 1070 Ti (2432 core, 1683 MHz, 8GB RAM).

3.2. Experiment results

Table 2. Anomaly detection efficiency of kernel functions on image set

	Uniform	Hypercube	Triangular	Epanechnikov	Quartic	Triweight	Tricube	Gaussian	Cosine
Ảnh 1	0.9982	0.9982	0.9981	0.9981	0.9981	0.9981	0.9981	0.9981	0.9981
Ảnh 2	0.9969	0.9969	0.9970	0.9970	0.9970	0.9970	0.9970	0.9969	0.9970
Ảnh 3	0.9691	0.9732	0.9732	0.9681	0.9732	0.9732	0.9732	0.9688	0.9732
Ảnh 4	0.9591	0.9591	0.9587	0.9587	0.9587	0.9587	0.9587	0.9588	0.9587
Ảnh 5	0.9887	0.9887	0.9881	0.9883	0.9883	0.9883	0.9884	0.9883	0.9883
Ảnh 6	0.9996	0.9996	0.9996	0.9996	0.9996	0.9996	0.9996	0.9996	0.9996
Average	0.9853	**0.9859**	0.9858	0.9850	0.9858	0.9858	0.9858	0.9851	0.9858

After the experiment process, we carry out evaluation and make recommendations

for appropriate kernel selection with three criteria: the anomaly detection efficiency; the complexity of algorithm, the complexity of storage space and implementation time duration; the complexity in bandwidth selection of kernel functions.

3.2.1. Anomaly detection efficiency: On an one-by-one basis, run the Algorithm 1 with 9 kernel functions in Table 1 for images described above, the anomaly detection efficiency is shown in Table 2. From these results, we see that the Hypercube kernel function delivers the best average efficiency for anomalous pixel detection, followed by Triangular, Quartic, Triweight, Tricube and Cosine kernel functions. Group of kernel functions with the worst efficiency for anomalous pixel detection include Epanechnikov, Gausian, and Uniform. However, the discrepancy in anomaly detection among kernel functions is very small (average discrepancy is less than 0.1%), so additional consideration has to be given to relevant issues such as implementation time duration, the complexity in bandwidth selection.

Table 3. Implementation time of kernel functions

	Time (s)
Uniform	1,568
Hypercube	**1,349**
Triangular	1,638
Epanechnikov	4,978
Quartic	4,307
Triweight	4,351
Tricube	4,661
Gaussian	22,239
Cosine	4,345

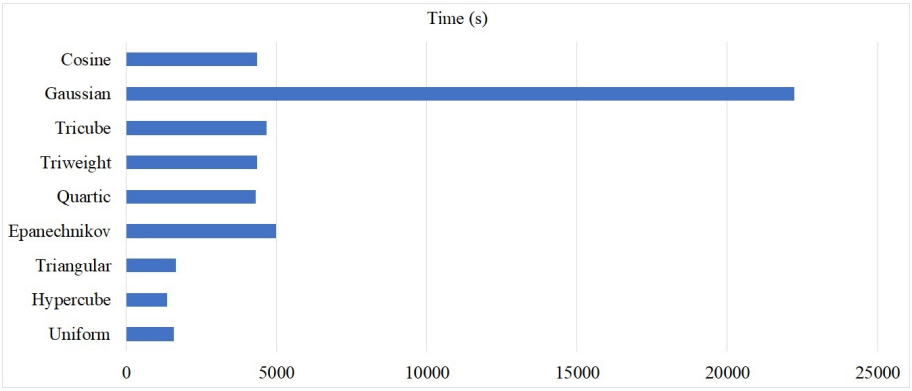

Fig. 7. Chart of implementation time of kernel functions.

3.2.2. Implementation time duration and complexity of algorithm: In Algorithm 1 we see that, the calculation complexity is $O(kn^2)$, the complexity of storage space is $O(n)$ for all kernel functions. However, regarding calculation time duration, by actual experiment on Image 1, using Algorithm 1 with 9 different kernel functions listed in Table 1 for calculation, the implementation time duration is shown in Table 3

and Fig. 7. Observing results for implementation time of kernel functions in Table 3 and Fig. 7, we notice that the Hypercube function has the least implementation time duration has the shortest implementation time, the Gaussian kernel function has the longest implementation time (16 times longer than the calculation time of Hypercube kernel function).

3.2.3. Impact of bandwidth: How to select bandwidth to achieve the highest anomalous pixel detection efficiency is currently the most challenging issue of this method. Among publications [5], [11], [13], [14] as mentioned above, there has not been any publication that discusses this issue. Maybe because author used the Gaussian kernel function, so by default, the selected bandwidth is $h = 1.06\sigma n^{-1/5}$ as recommended by Silverman [17]. In publications of: Hardle [10], Devroye and Gyorf [16], Silverman [17], Webb [18] and Scott [19], authors mentioned how to select bandwidth to smoothen the PDF function. However, only calculate bandwidth for Gaussian kernel function, other functions have not been mentioned.

Table 4. Bandwidths of kernel functions that enable algorimths to deliver highest anomaly detection efficiency

	Image 1	Image 2	Image 3	Image 4	Image 5	Image 6
Uniform	7	5	1	9	11	13
Hypercube	14	10	1	18	22	22
Triangular	10	8	1	12	20	15
Epanechnikov	4	3	1	5	8	7
Quartic	11	8	1	14	19	15
Triweight	13	10	1	16	22	18
Tricube	11	8	1	14	21	19
Gaussian	4	4	1	5	8	6
Cosine	9	7	1	12	16	13

In the experiment part on the sample data set, we applied the bandwidth calculation method posed by Silverman [17]; however, the anomaly detection efficiency of the algorithm on kernel functions is markedly lower than the highest anomaly detection efficiency shown in Table 2. The bandwidth for the algorithm to achieve the highest anomaly detection efficiency is shown in Table 4. Observing data in Table 4, we notice that there is no rule to select an appropriate bandwidth, for all kernel functions, that produces the best anomaly detection efficiency of the algorithm. It is also impossible to select one bandwidth for a kernel function that satisfies all images. Fig. 8, 9, 10, 11, 12, 13 show graphs of anomalous pixel detection efficiency of Algorithm 1 with 9 different kernel functions and bandwidth varying from 1 to 30, which correspond to the input data of Image 1, Image 2, Image 3, Image 4, Image 5, Image 6.

Next, we tested the influence of bandwidth to 9 kernel functions on anomaly detection efficiency, results are shown in Fig. 8, 9, 10, 11, 12 and 13. From testing results, we notice that the three curses representing anomaly detection efficiency of algorithm, which correspond with the three kernel functions Epanechnikov, Gaussian and Uniform, have relatively high gradient toward the right side. This means that: larger bandwidth

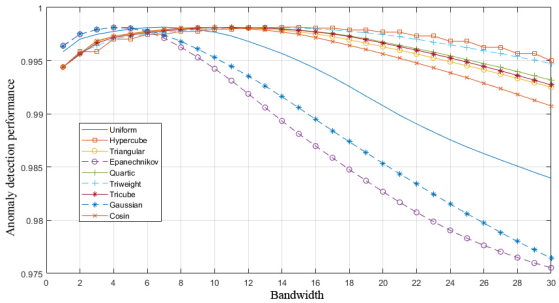

Fig. 8. The graph shows anomaly detection efficiency of Algorithm 1 on Image 1 using various kernel functions when bandwidths vary from 1 to 30.

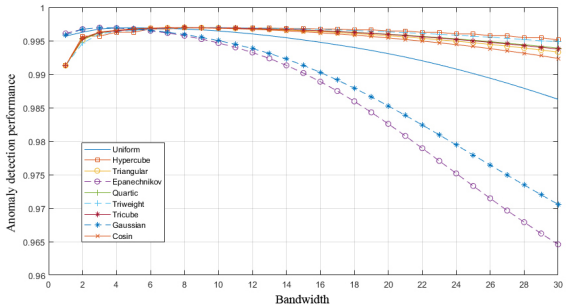

Fig. 9. The graph shows anomaly detection efficiency of Algorithm 1 on Image 2 using various kernel functions when bandwidths vary from 1 to 30.

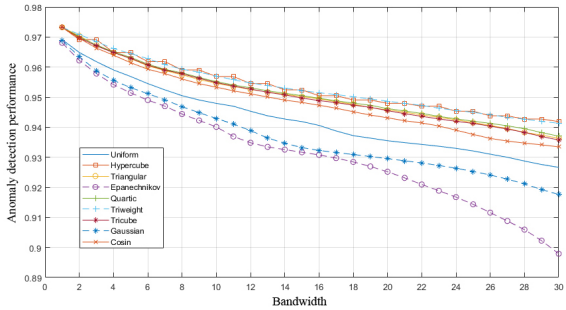

Fig. 10. The graph shows anomaly detection efficiency of Algorithm 1 on Image 3 using various kernel functions when bandwidths vary from 1 to 30.

delivers lower anomaly detection efficiency, and this efficiency decreases at a higher rate compared to the rest of kernel functions. The bandwidth range within which algorithm delivers anomaly detection efficiency around the maximum point is relatively short, making it difficult to find out the appropriate bandwidth. So with the short optimum bandwidth range and the decreasing rate of anomaly detection efficiency, it would be very difficult to determine an appropriate bandwidth value for Epanechnikov, Gaussian and Uniform kernel functions.

On the contrary to the three kernel functions above, the Triangular, Quartic, Tri-

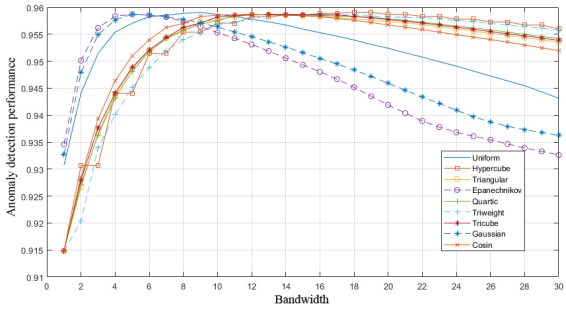

Fig. 11. The graph shows anomaly detection efficiency of Algorithm 1 on Image 4 using various kernel functions when bandwidths vary from 1 to 30.

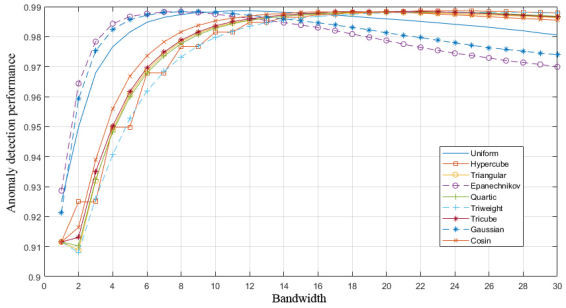

Fig. 12. The graph shows anomaly detection efficiency of Algorithm 1 on Image 5 using various kernel functions when bandwidths vary from 1 to 30.

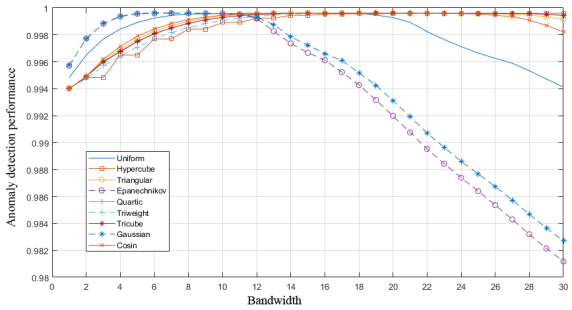

Fig. 13. The graph shows anomaly detection efficiency of Algorithm 1 on Image 6 using various kernel functions when bandwidths vary from 1 to 30.

weight, Tricube, Cosine and especially Hypercube kernel function has the low right-side gradient. The bandwidth range within which algorithm delivers anomaly detection efficiency around the maximum point is large, so it is more favourable to find and select an appropriate bandwidth compared to Epanechnikov, Gaussian and Uniform kernel functions.

From analysis on anomaly detection efficiency, calculation time and bandwidth finding and selecting of kernel functions, we notice that Hypercube kernel function has the marked advantage, followed by Triangular, Quartic, Triweight, Tricube, Cosine kernel

functions. Gaussian kernel function has been used widely in publications [5], [11], [13], [14] and not shown its advantage yet. The experiment on the sample data set also showed that Gaussian kernel function is the worst-performing kernel function (with 2nd lowest anomaly detection efficiency among 9 kernel functions, the longest calculation time and the most difficult bandwidth determination process).

4. Conclusions and Future works

In search and rescue operations, enhancing efficiency in detection of object in search or signals containing information about objects in search is ultimately critical. This will reduce time and financial expense, energy, as well as increase the rescue possibility. Applying Neyman-Pearson lemma based on kernel density estimation of background data to make decision is an effective and reliable technique for detection of anomalous pixel on UAV images in search and rescue operations. Numerous kernel functions have been published; however, there has not been any research discussing which kernel function to be used for this anomaly detection task. By using experimental method on the sample data set, carry out evaluation with two criteria (anomalous pixel detection efficiency; implementation time and complexity in calculation and storage); additionally, evaluate the favourability in selecting bandwidth, the Hypercube kernel function has the greatest advantage (deliver the best anomalous pixel detection efficiency, the shortest implementation time, large appropriate bandwidth range that facilitates bandwidth determination), followed by Triangular, Quartic, Triweight, Tricube, Cosine, the group of worst-performing kernel functions include Epanechnikov, Gaussian and Uniform.

Acknowledgment

The present research is financed by the national-level scientific research project no. VT-UD.04/16-20 of Space Science and Technology Program. Our group of authors would like to thank for the support and accompany of the Management Board of Space Science and Technology Program.

References

[1] T. G. of the Socialist Republic of Vietnam, *Decree No. 36/2008/ND-CP dated March 28, 2008 of the Government on management of unmanned aircraft and ultralight aircraft*, 2008.

[2] V. T. T. Bach. (2019) Unmanned aircraft and some basic concepts. [Online]. Available: https://vatm.vn/tau-bay-khong-nguoi-lai-va-mot-so-khai-niem-co-ban-n5358.html

[3] S. Grogan, R. Pellerin, and M. Gamache, "The use of unmanned aerial vehicles and drones in search and rescue operations – a survey," in *Conference: PROLOG 2018*, 2018, pp. 1–12.

[4] H. Shakhatreh, A. H. Sawalmeh, A. I. Al-Fuqaha, Z. Dou, E. K. Almaita, I. M. Khalil, N. S. Othman, A. Khreishah, and M. Guizani, "Unmanned aerial vehicles (uavs): A survey on civil applications and key research challenges," in *IEEE Access*, vol. 7, 2019, pp. 1–63.

[5] T. Bolukbasi and P. Tran, "Outline color identification for search and rescue," *Technical Reportof Department of Electrical and Computer Engineering, Boston University*, no. ECE-2012-07, 2012.

[6] M. Ramachandran and W. Moik, "Outline color identification for search and rescue," *Technical Reportof Department of Electrical and Computer Engineering, Boston University*, no. ECE-2013-03, 2013.

[7] T. Marshall and L. N. Perkins, "Color outline detection for search and rescue," *Technical Reportof Department of Electrical and Computer Engineering, Boston University*, no. ECE-2015-01, 2015.
[8] N. V. Phuong and D. K. Hoai, "Anomaly detection techniques on uav images for search and rescue," *Journal of Research and Development on Information and Communication Technology*, vol. V-1, no. 39, pp. 1–8, 2018.
[9] I. S. Reed and X. Yu, "Adaptive multiple-band cfar detection of an optical pattern with unknown spectral distribution," *IEEE transactions on acoustics. speech. and signal processing*, vol. 38, no. 10, pp. 1760–1770, 1990.
[10] W. Hardle, A. Werwatz, M. Muller, and S. Sperlich, *Nonparametric and Semiparametric Models*, 2004.
[11] T. Veracini, S. Matteoli, M. Diani, and G. Corsini, "Nonparametric framework for detecting spectral anomalies in hyperspectral images," *IEEE Geoscience and Remote Sensing Letters*, vol. 8, no. 4, pp. 666–670, 2011.
[12] E. Parzen, "On estimation of a probability density function and mode," *Annals of Mathematical Statistics*, vol. 33, pp. 1065–1076, 1962.
[13] S. Matteoli, T. Veracini, M. Diani, and G. Corsini, "Background density nonparametric estimation with data-adaptive bandwidths for the detection of anomalies in multi-hyperspectral imagery," *IEEE Geoscience and Remote Sensing Letters*, vol. 11, pp. 163–167, 2014.
[14] C. Zhao, X. Wang, and G. Zhao, "Detection of hyperspectral anomalies using density estimation and collaborative representation," *Remote Sensing Letters*, vol. 8, no. 11, p. 1025–1033, 2017.
[15] M. Rosenblatt, "Remarks on some nonparametric estimates of a density function," *The Annals of Mathematical Statistics*, vol. 27, no. 3, pp. 832–837, 1956.
[16] L. Devroye and L. Gyorfi, *Nonparametric Density Estimation: The L1 View*. Wiley, New York, 1985.
[17] B. W. Silverman, *Density Estimation for Statistics and Data Analysis*, 1986.
[18] A. R. Webb, *Statistical Pattern Recognition, Second Edition*, 2002.
[19] D. W. Scott, *Multivariate Density Estimation: Theory, Practice, and Visualization, 2nd Edition*, 2015.

Manuscript received 21-11-2019; Accepted 14-5-2020.

■

Nguyen Van Phuong graduated from Le Quy Don Technical University in 2003, received a master's degree from Le Quy Don Technical University in 2009. Currently a PhD student at the Faculty of Information Technology, Le Quy Don Technical University. Research field: GIS, optical remote sensing image processing. E-mail: phuongnv.dl@gmail.com

Dao Khanh Hoai received a PhD in 2005. Currently working at the Le Quy Don Technical University. Research field: GIS, satellite image processing, UAV, metering and computer vision. E-mail: geogroup2008@gmail.com

Tong Minh Duc graduated from Le Quy Don Technical University in 2000. Received a doctorate from University of Electrical Engineering - Russia in 2007. Currently a lecturer at the Faculty of Information Technology - Le Quy Don Technical University. Research field: Image processing, object identification, Information security safety. E-mail: ductm@mta.edu.vn

HIỆU SUẤT PHÁT HIỆN DỊ THƯỜNG TRÊN ẢNH UAV CỦA CÁC HÀM ƯỚC LƯỢNG MẬT ĐỘ HẠT NHÂN

Tóm tắt

Hiệu suất phát hiện các điểm ảnh dị thường trên ảnh UAV của các thuật toán được thể hiện trên hai tiêu chí: hiệu quả phát hiện các điểm ảnh dị thường (sử dụng diện tích dưới đường cong ROC để đánh giá) và thời gian tính toán. Một kỹ thuật phát hiện dị thường trên ảnh UAV rất hiệu quả đã được các nhà nghiên cứu đề xuất đó là áp dụng quy tắc Neyman–Pearson dựa trên việc tính toán hàm mật độ xác suất thông qua ước tính hàm mật độ hạt nhân (Kernel Density Estimation - KDE) của dữ liệu nền để đưa ra quyết định. Trong phương pháp này, việc lựa chọn hàm hạt nhân (kernel) và băng thông đóng vai trò quyết định đến hiệu suất phát hiện dị thường. Tuy nhiên, cho đến nay chưa có bất kỳ nghiên cứu nào đề cập đến vấn đề này. Vì vậy, trong bài báo này, chúng tôi đánh giá hiệu suất phát hiện dị thường trên ảnh UAV qua một số hàm hạt nhân thông dụng thường được trích dẫn trong các nghiên cứu cho KDE, từ đó đưa khuyến nghị sử dụng hàm hạt nhân phù hợp. Các thử nghiệm, đánh giá được thực hiện trên bộ dữ liệu mẫu được chụp trên các loại địa hình khác nhau và các đối tượng cần tìm kiếm khác nhau.